THE JOURNAL OF BIOLOGICAL CHEMISTRY VOL. 288, NO. 33, pp. 24035–24048, August 16, 2013

Planar Cell Polarity Pathway Regulates Nephrin Endocytosis in Developing Podocytes[S]

Received for publication, January 14, 2013, and in revised form, June 12, 2013 Published, JBC Papers in Press, July 3, 2013, DOI 10.1074/jbc.M113.452904

Sima Babayeva[‡], Brittany Rocque[‡1], Lamine Aoudjit[‡], Yulia Zilber[‡], Jane Li[‡], Cindy Baldwin[‡], Hiroshi Kawachi[§], Tomoko Takano[‡2], and Elena Torban[‡3]

From the [‡]Department of Medicine, McGill University, Montreal, Quebec, Canada H3A2B4 and the [§]Department of Cell Biology, Institute of Nephrology, Niigata University Graduate School of Medical and Dental Sciences, Niigata, Niigata Prefecture 950-2181, Japan

Background: The PCP pathway controls many cell processes during development.
Results: The PCP pathway induces nephrin endocytosis when cultured podocytes are treated with Wnt5a. Loss of PCP protein Vangl2 decreases nephrin endocytosis.
Conclusion: During glomerular development, endocytosis of nephrin is regulated by the PCP pathway.
Significance: Implicating the PCP pathway in nephrin endocytosis is important for understanding the complexity of PCP signaling during mammalian development.

The noncanonical Wnt/planar cell polarity (PCP) pathway controls a variety of cell behaviors such as polarized protrusive cell activity, directional cell movement, and oriented cell division and is crucial for the normal development of many tissues. Mutations in the PCP genes cause malformation in multiple organs. Recently, the PCP pathway was shown to control endocytosis of PCP and non-PCP proteins necessary for cell shape remodeling and formation of specific junctional protein complexes. During formation of the renal glomerulus, the glomerular capillary becomes enveloped by highly specialized epithelial cells, podocytes, that display unique architecture and are connected via specialized cell-cell junctions (slit diaphragms) that restrict passage of protein into the urine; podocyte differentiation requires active remodeling of cytoskeleton and junctional protein complexes. We report here that in cultured human podocytes, activation of the PCP pathway significantly stimulates endocytosis of the core slit diaphragm protein, nephrin, via a clathrin/β-arrestin-dependent endocytic route. In contrast, depletion of the PCP protein Vangl2 leads to an increase of nephrin at the cell surface; loss of *Vangl2* functions in *Looptail* mice results in disturbed glomerular maturation. We propose that the PCP pathway contributes to podocyte development by regulating nephrin turnover during junctional remodeling as the cells differentiate.

The noncanonical Wnt/planar cell polarity (PCP)[4] pathway refers to a fundamental evolutionarily conserved mechanism that establishes directional cell polarity essential for development of many tissues and organs (1). In vertebrates, PCP signaling is activated upon Wnt ligand binding to a Frizzled (Fz) receptor. In different cellular contexts, Wnt4 (2), Wnt5a (3), Wnt9b (4), and Wnt11 (5) have all been reported to activate the PCP pathway (6, 7); Wnt5a has emerged as the prototypical PCP Wnt ligand (8, 9). Wnt5a-Fz binding leads to the formation of asymmetrically positioned multiprotein complexes composed of the core PCP proteins Van Gogh-like (Vangl), Dishevelled, Prickle, Flamingo, and Diego; the functions of additional PCP proteins Fat and Dachsous are also needed to achieve planar tissue polarity (1). PCP protein complexes interact with the cell-cell junctions that act as the signaling hubs to propagate information from cell to cell (10). The asymmetric redistribution of PCP proteins is crucial for initiating a chain of signaling events that regulate the polarized protrusions that remodel the extracellular matrix and underlie collective directional cell movements (1). Importantly, these cellular processes are essential for kidney morphogenesis (7, 11, 12).

Loss of PCP function during development adversely affects morphogenesis of many organs including the kidneys (7). Homozygous mutations in *Fat4* (13), *Dachsous1* (14), or double *Fat1*/*Fat4* mutants (15) disturb renal tubular elongation and tubular dilation and cause embryonic renal cyst formation. Knockout of *Fat1* leads to the congenital nephrotic syndrome (16). In a mouse with a spontaneous homozygous mutation in the core PCP gene, *Vangl2* (*Looptail* mouse) (17, 18), defects in kidney branching morphogenesis and glomerular morphology and maturation were recently reported (19). In our earlier work, we identified a complete complement of PCP transcripts (including Vangl2) in cultured human podocytes and showed that knockdown of Vangl2 or stimulation with the PCP ligand Wnt5a of cultured podocytes induced actin cytoskeletal reorganization, affected cell migration, and changed the distribution of the podocyte protein, nephrin (20).

[S] This article contains supplemental Figs. 1–3.

[1] Supported by a Research Institute-McGill University Health Center graduate scholarship award.
[2] Supported by Canadian Institute of Health Research Operating Grant MOP-97759.
[3] Supported by Canadian Institute of Health Research Operating Grant MOP-102646. To whom correspondence should be addressed: Dept. of Medicine, McGill University, 3775 University St., Montreal, Quebec, Canada H3A2B4. Tel.: 514-398-8150; Fax: 514-398-7446; E-mail: elena.torban@mcgill.ca.

[4] The abbreviations used are: PCP, planar cell polarity; CHC, clathrin heavy chain; CM, conditioned medium; E*n*, embryonic day; Fz, Frizzled; PFA, paraformaldehyde; PMA, phorbol 12-myristate 13-acetate; OPD, *o*-phenylenediamine; SD, slit diaphragm; Vangl, Van Gogh-like.

Nephrin is an immunoglobulin-like transmembrane protein (21). In adult kidneys, nephrin expression is restricted to the visceral glomerular podocytes. Nephrin is uniquely localized to the slit diaphragm (SD) junctional contacts between adjacent podocytes which form the filtration barrier which restricts passage of protein into ultrafiltrate. At the SD, the extracellular domains of nephrin from adjacent podocytes interact with each other in a counterparallel manner and serve as the SD structural backbone (21, 22). The cytoplasmic portion of nephrin is linked to the podocyte cytoskeleton via a number of adaptor proteins (23); *nephrin* gene mutations lead to profound changes of the podocyte cytoskeleton, loss of SD junctions, and proteinuria (24). It is believed that SDs undergo continuous remodeling in response to physiologic changes in filtration pressure (25). Quack *et al.* demonstrated that threonine phosphorylation of nephrin triggers recruitment of β-arrestin-2, an adaptor protein known to mediate endocytosis of G protein-coupled receptors (26), which induces nephrin endocytosis (27). Nephrin internalization was also shown to occur via CIN85-mediated ubiquitination (28) and raft-mediated endocytosis (29). So far, disturbances of nephrin endocytosis have been implicated in the context of disease states, for example in high glucose-mediated podocyte injury (27). However, nephrin turnover during glomerular development has not been studied, and the role of the noncanonical Wnt/PCP pathway in nephrin endocytosis has not been addressed.

The purpose of the current work was to ascertain whether the PCP pathway regulates subcellular localization of nephrin during podocyte differentiation and to study its cellular mechanisms. We show that Wnt5a stimulates nephrin endocytosis via a clathrin/β-arrestin-dependent route. We also reveal an important role for Vangl2 in nephrin internalization and subcellular distribution.

EXPERIMENTAL PROCEDURES

Animal Husbandry and Embryo Harvest—Looptail (*Vangl2*$^{lp/+}$) mice (17) were generously provided by Dr. Gros (McGill). All animal manipulations were according to the Canadian Animal Act and were approved by the McGill University Animal Care Committee (ACC Protocol 5423). Heterozygous *Lp* mice were sister-brother-mated to obtain homozygous embryos; a morning plug after overnight mating was counted as 0.5 day *postcoitum* (embryonic day E0.5). At E17.5, pregnant dams were euthanized, and embryos were dissected, washed in phosphate-buffered saline, and fixed in 4% paraformaldehyde (PFA). Additional C57BL/6 control animals were bred to obtain E17.5 embryonic tissues for protein localization studies. All embryos were either cryopreserved in OCT compound for Vangl2 staining or dehydrated in 25, 50, and 75% ethanol and paraffin embedded at the Goodman Cancer Center Histology Service, McGill University.

Cell Cultures—Human podocytes A8/13 (30) (gift from Dr. M. Saleem), were propagated and differentiated on coverslips in 12-well plates prior to treatment and staining as described previously (20). Human embryonic kidney HEK293 cells stably transfected with full-length rat nephrin expression construct (HEK293/N) have been characterized previously (31). HEK293/N cells were grown on coverslips in 12-well plates or 24-well plates in DMEM supplemented with 10% FBS, 1% penicillin/streptomycin solutions (all from Wisent Inc.), and hygromycin (Bishop) for 72 h followed by incubation with the conditioned medium collected from L-Wnt5a-expressing cells (ATCC CRL-2814) or paternal control L cells (ATCC CRL-2648) for various times as indicated under "Results." L and L-Wnt5a cells were grown as recommended by the ATCC. In some experiments, HEK293/N cells (5×10^5/well) were grown in 12-well plates for 24 h and transfected with 100 ng/well human Rab5-GFP, Rab7-GFP (both kindly provided by Dr. Gruenheid), or human Rab11-GFP (Addgene). After 48 h, cells were incubated with L-CM or Wnt5a-CM for various periods of time. The cells were fixed and processed for immunofluorescent microscopic studies.

siRNA and shRNA Interference Assays—1×10^5 HEK293/N cells/well were grown in 24-well plates under the conditions described above. The next day, cells were transfected with 20 pmol of either control (Santa Cruz Biotechnology sc-37007) or a pool of three anti-human Vangl2 siRNAs (Santa Cruz Biotechnology sc-45595) by using Lipofectamine 2000 (Invitrogen) as described by the manufacturer. After a 6-h incubation with siRNAs, medium was replaced with fresh DMEM, and cells were incubated for additional 48 h. The shRNAs targeting β-arrestin-1 and β-arrestin-2 (provided by Dr. Stefane Laporte, McGill) were described previously (32). The siRNAs targeting human clathrin heavy chain (provided by Dr. Peter McPherson, McGill) were described previously (33). The HEK293/N cells with depleted expression of genes of interest were processed for ELISA of nephrin internalization as described below.

For quantitative RT-PCR or immunoblotting analysis, 2×10^5 HEK293/N cells were grown in 35-mm plates, transfected with respective siRNAs or shRNAs as above, and collected 48–72 h after transfection. RNA was extracted with TRIzol (Sigma) as described by the manufacturer. Quantitative RT-PCR analysis to detect depletion of Vangl2 was carried with iTAG SYBR Green Super Mix kit (Bio-Rad) as described by the manufacturer. The following Vangl2 primers were used: Vangl2 forward, cttcctgaaggtgcctcttg; Vangl2 reverse, gtgaggtcatcatgggaga.

Immunofluorescent Studies—To detect endogenous nephrin expression in cultured human podocytes, A8/13 cells differentiated for 2 weeks were treated with L (control)- or Wnt5a-CM for 6 h. The cells were fixed in 4% PFA for 15 min at 4 °C, permeabilized with 0.5% Triton X-100 in PBS, and blocked with 10% normal goat serum (Jackson ImmunoResearch Laboratories) and 0.1% Triton X-100 in PBS at room temperature. The cells were labeled with polyclonal rabbit anti-nephrin antibody that recognizes the nephrin cytoplasmic domain (31) followed by secondary anti-rabbit IgG Alexa Fluor 488 antibody (Molecular Probes). Actin was detected by Alexa Fluor 568-conjugated phalloidin staining (Molecular Probes). Quantification of nephrin immunofluorescence intensity in the podocyte cortical zones was carried out with ImageJ software (Arch Version, ImageJ-win32) as described in supplemental Fig. 1.

For detection of rat nephrin, live HEK293/N cells were incubated for 1 h at 37 °C with a monoclonal antibody (mAb 5-1-6) (2.5 μg/ml) that recognizes the nephrin extracellular domain (31) followed by incubation with either Wnt5a-CM or L-CM

for 20 or 60 min at 37 °C. Attempts to label cells with mAb 5-1-6 at 4 °C or at room temperature were ineffective. Cells were then fixed and blocked in 0.5% Triton-X-100 containing solutions as above. For images shown in Fig. 3*A*, the 0.5% Triton X-100 permeabilization step was omitted. Nephrin was visualized with the anti-mouse IgG Alexa Fluor 488 or Cy3 (both Molecular Probes). Z-projections of immunostained podocytes or HEK293/N cells were captured with the AxioObserver-100 microscope (Zeiss) using AxioVision 4.8 software.

5-μm cryosections of the E17.5 wild-type C57BL/6 embryos were postfixed for 5 min in 4% PFA, boiled in citrate buffer for 2 min, and blocked in 10% normal goat serum for 1 h. Sections were incubated with polyclonal rabbit anti-Vangl2 (1:20) (34) at 4 °C overnight followed by incubation with guinea pig anti-nephrin antibody (1:150, Acris) for 1 h at room temperature. Primary antibodies were visualized with goat anti-rabbit Cy3 and anti-guinea pig Alexa Fluor 488 (Molecular Probes), respectively.

Paraffin-embedded 4-μm sections were deparaffinized by standard histological methods using xylene and various ethanol concentrations. Sections were boiled in citrate buffer, blocked as above, and incubated with rabbit anti-WT1 antibody (1:400, Santa Cruz Biotechnology) and guinea pig anti-nephrin antibody (1:50, Acris) followed by incubation with the secondary goat anti-rabbit Cy3 and anti-guinea pig Alexa Fluor 488 antibodies, respectively. Nuclei were stained with 4′,6-diamidino-2-phenylindole (DAPI, Invitrogen). All sections were mounted in Prolong Gold Antifade (Molecular Probes). All images of developing glomeruli were taken on a LSM 780 Laser Scanning Confocal Microscope (Zeiss) at the Imaging Core Facility of the Research Institute of the McGill University Health Centre (RI-MUHC) using the Plan-Apochromat 63×/1.40 N.A. oil differential interference contrast objective. Lasers used were argon multilines 488 nm (green), diode-pumped solid state (DPSS) DPSS 561 nm (red), diode 405 nm (DAPI) with Zen 2010 software for image acquisition.

Protein Interaction Assays and Immunoblotting—The HEK293T cells grown in 100-mm plates were co-transfected with 5 μg of yellow fluorescent protein (YFP)-tagged β-arrestin-2 and 5 μg of pCDM8-human IgG or 5 μg of pCDM8-human IgG-NephrinC using a Calcium Phosphate Transfection kit (Invitrogen) according to the manufacturer's instructions. 24 h after transfection, cells were stimulated with L- or Wnt5a-CM for 3 h. Cells were lysed in buffer containing 1% Triton X-100, 125 mM NaCl, 10 mM Tris (pH 7.4), 1 mM EDTA, 1 mM EGTA, 2 mM Na_3VO_4, 10 mM sodium pyrophosphate, 25 mM NaF, and protease inhibitor mixture (Roche Diagnostics). Pulldown assays were performed with 1 mg of cell lysate/condition mixed with 30 μl of protein G-Sepharose (Invitrogen). Precipitates were separated by SDS-PAGE, transferred to nitrocellulose membrane, blocked with 5% dry milk, and incubated with rabbit anti-GFP (Santa Cruz Biotechnology) or anti-nephrin (31) primary antibodies for 16 h at 4 °C followed by incubation with goat anti-rabbit horseradish peroxidase-conjugated secondary antibodies (Medicorp Inc.) and detection by enhanced SuperSignal West Pico chemiluminescence (Thermo Scientific).

HEK293/N cells were incubated with either L-CM or Wnt5a-CM medium for 1, 2, and 6 h. Cells were treated in the lysis buffer used for pulldown experiments. 25 μg of protein/lane was separated on 8% SDS-PAGE and subjected to immunoblot analysis with rabbit anti-nephrin antibody (31) or rabbit anti-β-catenin antibody (Santa Cruz Biotechnology) and secondary HRP-conjugated antibody as in the pulldown experiments above. As a control for loading variation, immunoblotting with anti-GAPDH antibody (Santa Cruz Biotechnology) was used.

For si/shRNA-mediated depletion experiments, HEK293/N cells were lysed in the buffer as above, and 50 μg of lysates was separated by 8% SDS-PAGE and transferred to nitrocellulose. The depletion of β-arrestin-1/2 was detected with rabbit pan-anti-β-arrestin antibody (32). The clathrin heavy chain was detected with rabbit anti-clathrin heavy chain antibody (33), and protein loading was monitored by the detection with mouse anti-α-tubulin antibody (Sigma-Aldrich). Band intensities corresponding to protein expression were quantified with AlphaImager EP (AlphaInnotech).

Analysis of Nephrin Internalization by ELISA—To measure nephrin internalization, we used an ELISA method described in Ref. 35 with some modifications. Briefly, HEK293/N cells were grown to 100% confluence in quadruplicate for each condition in 24-well plates. In each experiment, 4 wells were dedicated to the negative control (no antibodies). To detect nephrin at the cell surface, live HEK293/N cells were quickly washed in Hanks' balanced saline solution buffer (125 mM NaCl, 5 mM KCl, 2 mM $CaCl_2$, 1.2 mM $MgSO_4$, 25 mM HEPES) followed by a 20-min wash in Ca^{2+}-free medium at 37 °C. The cells were incubated with mAb 5-1-6 (2.5 μg/ml) in either L-CM or Wnt5a-CM for 1 h at 37 °C. Cells were washed four times in Hanks' balanced saline solution buffer and fixed for 10 min in 4% PFA followed by 10-min blocking in 5% skim milk/PBS at room temperature. The fixed cells were incubated with HRP-conjugated anti-mouse antibody (1:3000, Medicorp Inc.) for 1 h at room temperature followed by a detection step with freshly prepared *o*-phenylenediamine (OPD) substrate (Thermo Scientific) as recommended by the manufacturer. Final yellow-orange OPD-soluble products formed in each well were detected at 492 nm by ELISA Microplate reader ELx808 (Bio-Tec Instruments Inc.). In some parallel experiments, cells were incubated with phorbol 12-myristate 13-acetate (PMA, 250 ng/ml, Sigma-Aldrich) for 1 h at 37 °C (instead of L- or Wnt5a-CM). In some experiments, HEK293/N cells were preincubated with 0.4 nM PKCα inhibitor, bisindolylmaleimide I (EMD Millipore), for 30 min at 37 °C prior to incubation with Wnt5a-CM or L-CM or PMA and mAb 5-1-6.

To measure the total amount of nephrin, HEK293/N cells grown in parallel under the same conditions were incubated with either Wnt5a- or L-CM for 1 h at 37 °C and then fixed for 10 min in 4% PFA and permeabilized for 30 min in 0.1% Triton X-100/PBS at room temperature. The cells were blocked as above and incubated with the mAb 5-1-6 for 1.5 h followed by HRP-secondary antibody and OPD detection as above. Nephrin at the cell surface was normalized for both negative control (that was subtracted from the raw OPD data) and the total nephrin (that was used to calculate percentage of nephrin-pos-

itive signal detected in live un-permeabilized cells). The amount of internalized nephrin was calculated as a difference between 100% and the percentage of the normalized nephrin measured at the cell surface. The effect of Wnt5a *versus* control (L)-induced nephrin internalization in the majority of experiments was presented as a Wnt5a/L ratio of the percentages of internalized normalized nephrin. For each set of conditions, the experiments were repeated a minimum of three times in quadruplicate.

Statistical Analysis—The Student *t* test (two-tailed unequal variance) was used to calculate statistical significance in all graphs except Fig. 7. Mean ± S.E. are shown in all graphs. In Fig. 7, a χ^2 test was used.

RESULTS

Expression of PCP Protein Vangl2 in Developing Podocytes—We previously reported that the central PCP pathway protein, Vangl2, is expressed in developing podocytes in the mouse embryonic kidney (20), suggesting a role for PCP signaling during podocyte development. However, the dynamics of Vangl2 expression in podocytes as they undergo differentiation has not been studied, yet it might give a clue as to the function of the PCP pathway in glomerulogenesis. In mice, development of the glomerulus starts at ~E12.5 as renal mesenchyme converts into epithelium sequentially forming vesicles, comma- and S-shaped bodies. The proximal part of the S-shaped body gives rise to the future glomerulus that, at the early stage, is seen as a single loop-like structure enveloped by a row of cuboidal epithelial cells (early capillary loop-stage). As glomerulus matures, the capillary loop arrangement becomes progressively more complex with podocytes distributed in a less organized fashion (late capillary loop-stage) (36).

In sections of E17.5 mouse kidney, glomeruli at various developmental stages can be observed. Podocyte marker nephrin becomes detectable at the late S-shaped body to early capillary loop-stage along the lateral and basal aspects of cuboidal epithelial cells As the podocytes mature, nephrin at the lateral membrane descends toward the basal aspect of podocyte where the tight junctions are being reorganized into SDs (Fig. 1, *capillary loop-stage panels*, *magnified images*, *arrows*), as reported previously (37). We observed that Vangl2 expression in podocytes precedes that of nephrin: strong Vangl2 expression was observed along the basal-lateral plasma membrane of cuboidal epithelial cells in comma- and S-shaped bodies (Fig. 1, *top two rows*). At the capillary loop-stage, Vangl2 expression descends basally, and both nephrin and Vangl2 localize to the basal aspect of the podocyte where foot processes and SDs are formed (Fig. 1, *loop-stage panels*, *arrowhead*). At later developmental stages (>3 capillary loops) as podocytes mature and express higher levels of nephrin, Vangl2 expression is downregulated and can be visualized only under high acquisition exposure (Fig. 1, *maturing glomerulus panels*). Other PCP proteins (*e.g.* Fz 3 and Celsr 2) can also be detected in developing kidney (supplemental Fig. 3). Vangl2 mRNA, however, can be detected by RT-PCR in adult kidneys, glomeruli, and mouse and human podocyte cultures (20). By immunoblotting, Vangl2 protein can be detected in the adult mouse kidney (38).

Wnt5a Treatment of Cultured Human Podocytes Leads to Nephrin Internalization—Because in developing podocytes Vangl2 expression co-localizes with nephrin where the future slit diaphragm is being formed, we hypothesized that activation of the PCP pathway might be involved in discrete nephrin localization during slit diaphragm assembly. Because the PCP pathway is activated by Wnt5a *in vitro* (39), we incubated differentiated human podocytes with conditioned medium (CM) from L cells expressing Wnt5a or control L cells (L). Whereas the podocytes exposed to L-CM displayed nephrin in cell surface protrusions (Fig. 2*A*-B, *upper panels*), podocytes incubated with Wnt5a-CM showed striking redistribution of nephrin from the cell surface to the cytoplasm (Fig. 2, *A* and *B*, *lower panels*). Intensity of nephrin immunofluorescence in the cortical area of Wnt5a-CM-treated cells (9.76 ± 0.31 fluorescence intensity units/μm^2) was significantly lower than that in the cells treated with L-CM (22.49 ± 1.06) (Fig. 2*C* and supplemental Fig. 1).

We also examined this phenomenon in a second cell system. In HEK293 cells stably transfected with full-length rat nephrin (HEK293/N), nephrin localization was assessed by live cell labeling with mouse anti-nephrin antibody 5-1-6 (mAb 5-1-6) that recognizes the extracellular domain of rat nephrin (31). In the cells exposed to L-CM for 30 or 60 min, a strong nephrin signal (detected without detergent) was seen at the plasma membrane (Fig. 3*A*, *left panel*, 60-min incubation is shown). However, surface nephrin staining was markedly reduced in cells exposed to Wnt5a-CM (Fig. 3*A*, *right panel*). In the Wnt5a-CM-treated cells permeabilized with 0.1% Triton X-100, nephrin staining appeared in cytoplasmic vesicles (Fig. 3*B*, *right panel, arrowheads*). We then quantified plasma membrane nephrin (labeled in live cells) by ELISA, normalized for total nephrin (labeled in fixed cells). We found that only 8 ± 4.7% of total nephrin was present in the cytoplasm of L-CM-treated cells whereas 51 ± 5.1% of nephrin was internalized after a 1-h incubation with Wnt5a-CM (Fig. 2*C*).

To better understand the dynamics of Wnt5a-induced nephrin internalization, we used a panel of endosomal markers: Rab5 (early sorting endosomes), Rab7 (late endosomes, early lysosomes), and Rab11 (recycling endosomes). HEK293/N cells were transfected with GFP-tagged Rab cDNAs; 48 h later cells were live-labeled with mAb 5-1-6 and then exposed to L-CM or Wnt5a-CM for 20 or 60 min. In the L-CM-treated cells, nephrin resided predominantly at the cell surface at all time points (Fig. 4, *A–C*, all *L-CM images*). In Wnt5a-treated cells, we detected nephrin in the $Rab5^+$ vesicles at both 20- and 60-min time points (Fig. 4*A*, *right panels*). We did not see nephrin localization in recycling $Rab11^+$ endosomes at either 20 or 60 min (Fig. 4*B*, *right panels*). Occasionally, we saw nephrin in $Rab7^+$ vesicles (Fig. 4*C*, *right panels*). The presence of nephrin in $Rab7^+$ vesicles suggested that nephrin might be targeted for degradation. However, we detected no change in overall nephrin levels of HEK293/N cells incubated with Wnt5a-CM for 1–6 h (Fig. 4*D*).

Wnta5 Stimulates Clathrin-dependent Nephrin Endocytosis—Wnt5a was reported to induce endocytosis of the Fz4 receptor via a clathrin-dependent pathway (40). To examine whether Wnt5a stimulates nephrin endocytosis by a similar mechanism,

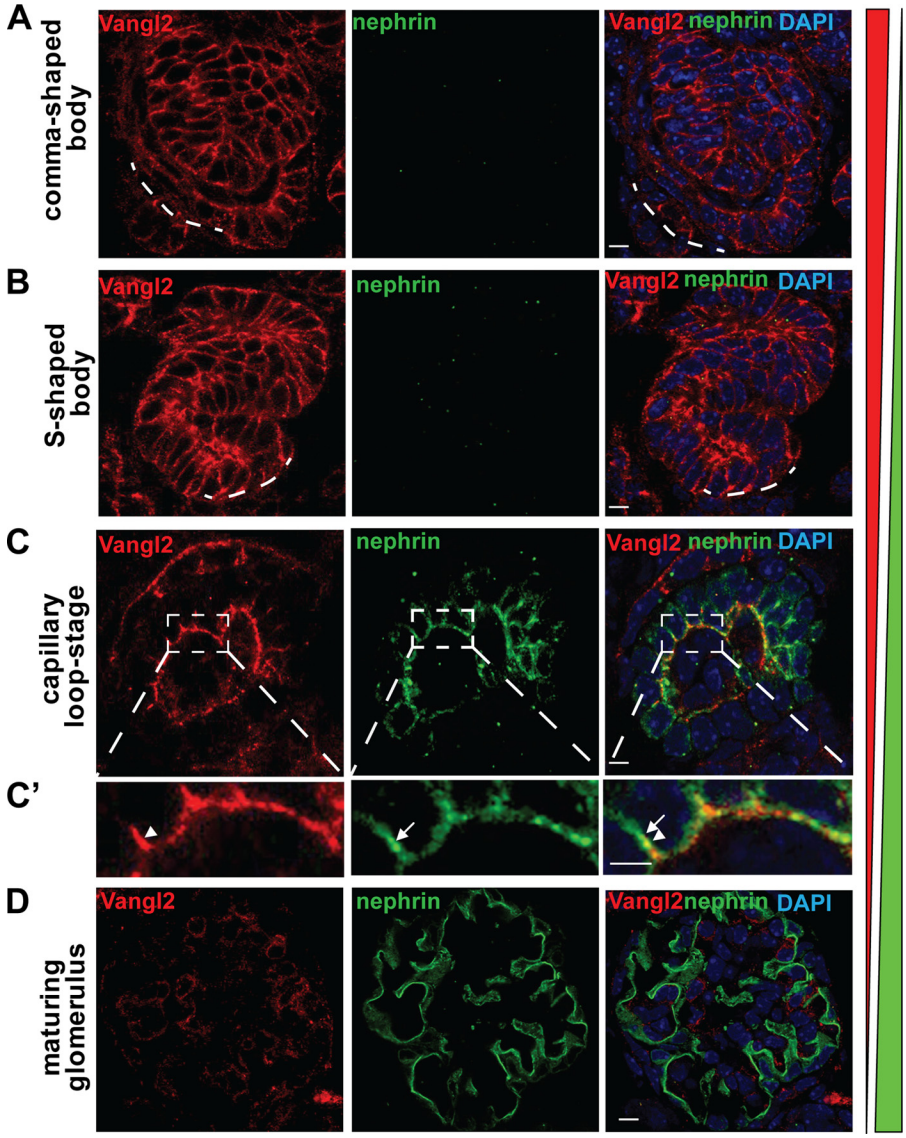

FIGURE 1. **Vangl2 is co-expressed with nephrin in developing podocytes.** E17.5 C57BL6 mouse sections co-stained with rabbit anti-Vangl2 (*red*) and guinea pig anti-nephrin antibodies (*green*), nuclei are revealed by DAPI (*blue*). *A*, Vangl2 expression (*red*) in comma-shape body. *Broken line* denotes the most proximal domain which will give rise to future podocytes. *B*, Vangl2 protein expression (*red*) in S-shaped body. *Broken line* denotes the most proximal domain of S-shape body where the future podocytes originate. *C*, glomerulus at the early capillary loop-stage. Vangl2 is expressed at the baso-lateral domain of podocytes (*red*), nephrin (*green*) co-localized with Vangl2 at the baso-lateral domain of podocyte plasma membrane. *C'*, high power view of the selected area in *box C*. Vangl2 (*red*, *arrowhead*) co-localizes with nephrin (*green*, *arrow*). *D*, maturing glomerulus. Vangl2 (*red*) expression is low, nephrin (*green*) is detected as a thin multi-looped line along the basal domain of podocyte plasma membrane. *Scale bar*, 5 μm.

HEK293/N cells were pretreated (30 min) with 0.45 mM sucrose (41) to inhibit clathrin-dependent endocytosis prior to incubation with Wnt5a- or L-CM. Sucrose treatment led to retention of nephrin at the cell surface (Fig. 5*A*). ELISA quantification revealed a significant ($p < 0.01$) decrease in Wnt5a-stimulated nephrin endocytosis, from 3.53 ± 0.18 to 2.02 ± 0.43-fold Wnt5a/L stimulation in cells exposed to sucrose (Fig. 5*B*). To confirm this effect, we analyzed Wnt5a-stimulated nephrin endocytosis after depletion of clathrin heavy chain (CHC) with specific anti-CHC siRNAs (33); we achieved ~70% depletion of CHC protein expression with specific siCHC RNAs compared with the base-line CHC protein levels in mock- or control siRNA-transfected HEK293/N cells (Fig. 5*D*). Wnt5a-induced nephrin internalization was reduced from 3.60 ± 0.13-fold stimulation in cells transfected with control siRNAs to 1.68 ± 0.26-fold stimulation after CHC knockdown (Fig. 5*C*). These results indicate that Wnt5a-induced nephrin endocytosis is mediated by a clathrin-dependent mechanism.

Wnt5a-induced Nephrin Internalization Is Mediated by β-Arrestin—Endocytosis via the clathrin-coated pit mechanism requires the multifunctional adaptor proteins, β-arrestins (42, 43). Both β-arrestin-1 and -2 are expressed in podocytes (44); β-arrestin-2 has been shown to interact with nephrin and to mediate clathrin-dependent nephrin endocytosis (27, 44). β-Arrestin-2 was also implicated in Wnt5a-induced endocytosis of Fz4 (40). We, therefore, tested whether Wnt5a-dependent endocytosis of nephrin requires β-arrestin. HEK293/N cells were transfected with control, β-arrestin-2, or with a combination of both β-arrestin-1/2 shRNAs. β-Arrestin-1 and -2 shRNAs showed some degree of cross-reactivity, and the com-

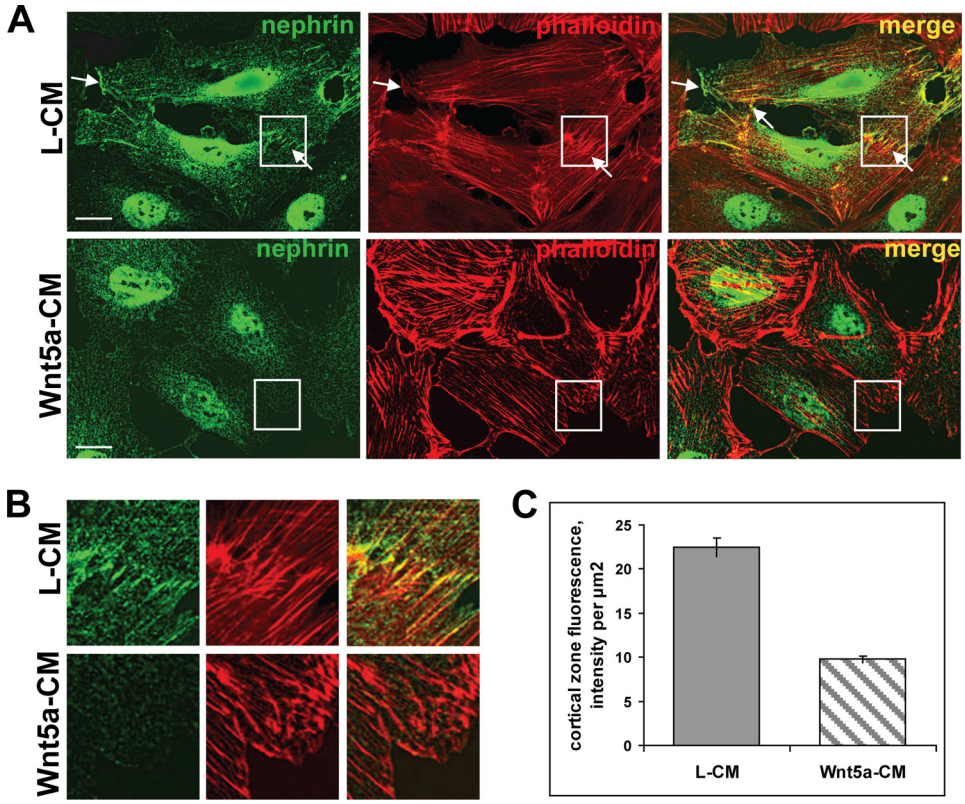

FIGURE 2. **Wnt5a induces nephrin redistribution from cell surface in human podocytes.** *A*, Wnt5a-induced redistribution of nephrin from cell projections (*arrows*) to the cytoplasm in cultured differentiated human podocytes; nephrin (*green*, visualized with rabbit anti-nephrin antibody), actin (*red*, visualized by Alexa Fluor 568-conjugated phalloidin). *Scale bar*, 5 μm. *B*, magnified imaged of cell area designated by *white boxes* in *A*. *C*, quantification of the fluorescent intensity corresponding to nephrin (detected with rabbit anti-nephrin antibody, *green*) in the cell cortical areas. 40 podocyte images per condition were analyzed by ImageJ software and normalized for the surface area as immunofluorescence intensity/μm^2. Mean $\pm$ S.E. (*error bars*) are shown, $p = 2.04E^{-15}$ (see also supplemental Fig. 1).

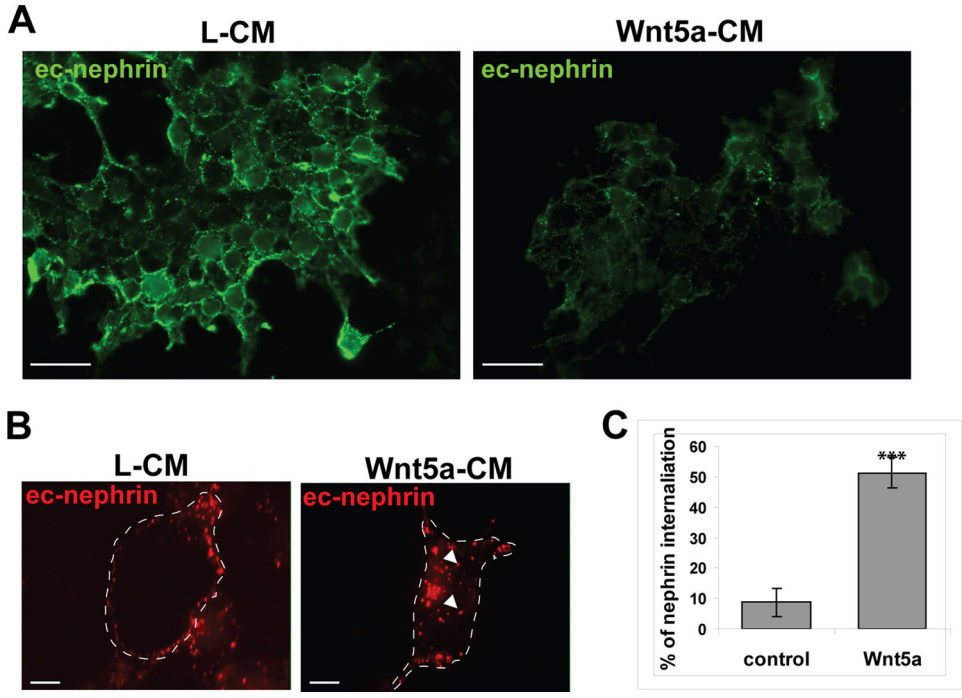

FIGURE 3. **Wnt5a induces nephrin endocytosis in HEK293 cells.** *A*, HEK293/N cells were live-labeled with anti-nephrin mAb 5-1-6 antibody (*green*) that recognizes nephrin ectodomain, then incubated for 60 min with L-CM (*left*) or with Wnt5a (*right*) and visualized with secondary antibody applied without permeabilization. *Scale bar*, 40 μm. *B*, cell surface regions of HEK293/N cells live-labeled with mAb 5-1-6 (*red*) and visualized with secondary antibody applied in the presence of detergent; *left image* shows cells treated with control L-CM for 60 min; *right image* shows cells treated with Wnt5a-CM; fluorescent signals are found in the cytoplasm (*arrowheads*) *C*, ELISA of nephrin internalization in HEK293/N cells. ***, $p < 0.0001$. *Error bars*, S.E.

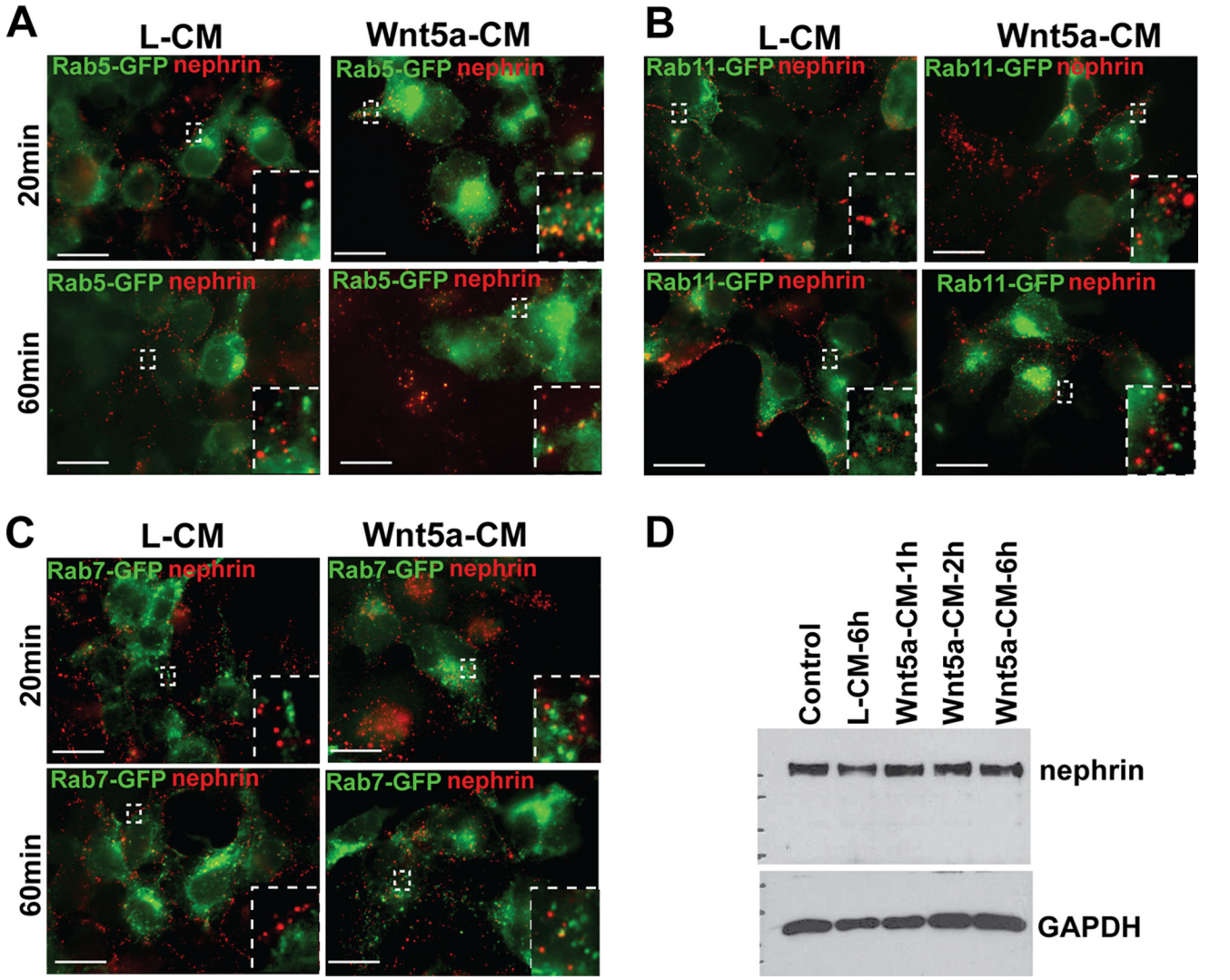

FIGURE 4. **Wnt5a induces nephrin localization to endocytic vesicles.** *A*, HEK293/N cells transfected with Rab5-GFP were live-labeled with mAb 5-1-6 (*red*) and then exposed to L- or Wnt5a-CM for 20 or 60 min; each *inset* shows a magnified image of the area indicated in the low magnification image. *B*, HEK293/N cells were transfected with Rab11-GFP and then processed as in *A*. *C*, HEK293/N cells were transfected with Rab7-GFP and then processed as in *A*. All *scale bars* are 5 μm. *D*, Western immunoblotting of nephrin in the HEK293/N cells exposed to either L or Wnt5a for indicated periods of time was performed. Control is the untreated cells. GAPDH levels in the same lysates served as loading controls.

bination of the two resulted in a more effective knockdown of β-arrestins than β-arrestin-2 alone (Fig. 6, *C* and *D*). 72 h after transfection, the cells were live-labeled with mAb 5-1-6 in the presence of either Wnt5a- or L-CM as above. In shControl-transfected cells exposed to Wnt5a, we detected nephrin mostly in the cytoplasm; little immunoreactive nephrin was noted at the cell surface (Fig. 6*A*, *left panel*). In contrast, knockdown of β-arrestins-1/2 led to retention of nephrin at the cell surface after exposure to Wnt5a (Fig. 6*A*, *right panel*). When quantified by ELISA, we observed 3.27 $\pm$ 0.32-fold stimulation of nephrin endocytosis in cells transfected with shControl and treated with Wnt5a. Although a similar level of Wnt5a-stimulated endocyosis (3.14 $\pm$ 0.63-fold) was seen in cells transfected with β-arrestin-2 shRNA alone, cells transfected with shRNA against both β-arrestins-1/2 displayed a significantly reduced Wnt5a-induced nephrin internalization to 1.84 $\pm$ 0.11-fold (Fig. 6*B*).

Under conditions that stimulate nephrin internalization (*e.g.* high glucose in diabetes mellitus), an increase in nephrin endocytosis was accompanied by an increase in β-arrestin-2/nephrin interaction (27). We, therefore, tested whether Wnt5a promotes complex formation between nephrin and β-arrestin-2. We took advantage of a chimeric construct (Ig-nephrin), in which an extracellular domain of human immunoglobulin is fused with the cytoplasmic domain of human nephrin (45). HEK293 cells were co-transfected with YFP-tagged β-arrestin-2 and either Ig-control (no nephrin) or Ig-nephrin. Transfected cells were treated with L- or Wnt5a-CM or PMA (that served as a positive control (27)). Ig-nephrin was then absorbed by affinity chromatography. As shown in Fig. 6*E*, there was a modest interaction between nephrin and β-arrestin-2 in control (Fig. 6*E*, *third lane*), however, this interaction was markedly increased when cells were stimulated with either Wnt5a (Fig. 6*E*, *fourth lane*) or PMA (Fig. 6*E*, *fifth lane*).

It has been reported that nephrin-β-arrestin-2 complex formation and nephrin endocytosis are facilitated under certain conditions by protein kinase Cα (PKCα) (27). During embryonic vascular development, Wnt5a was also reported to activate

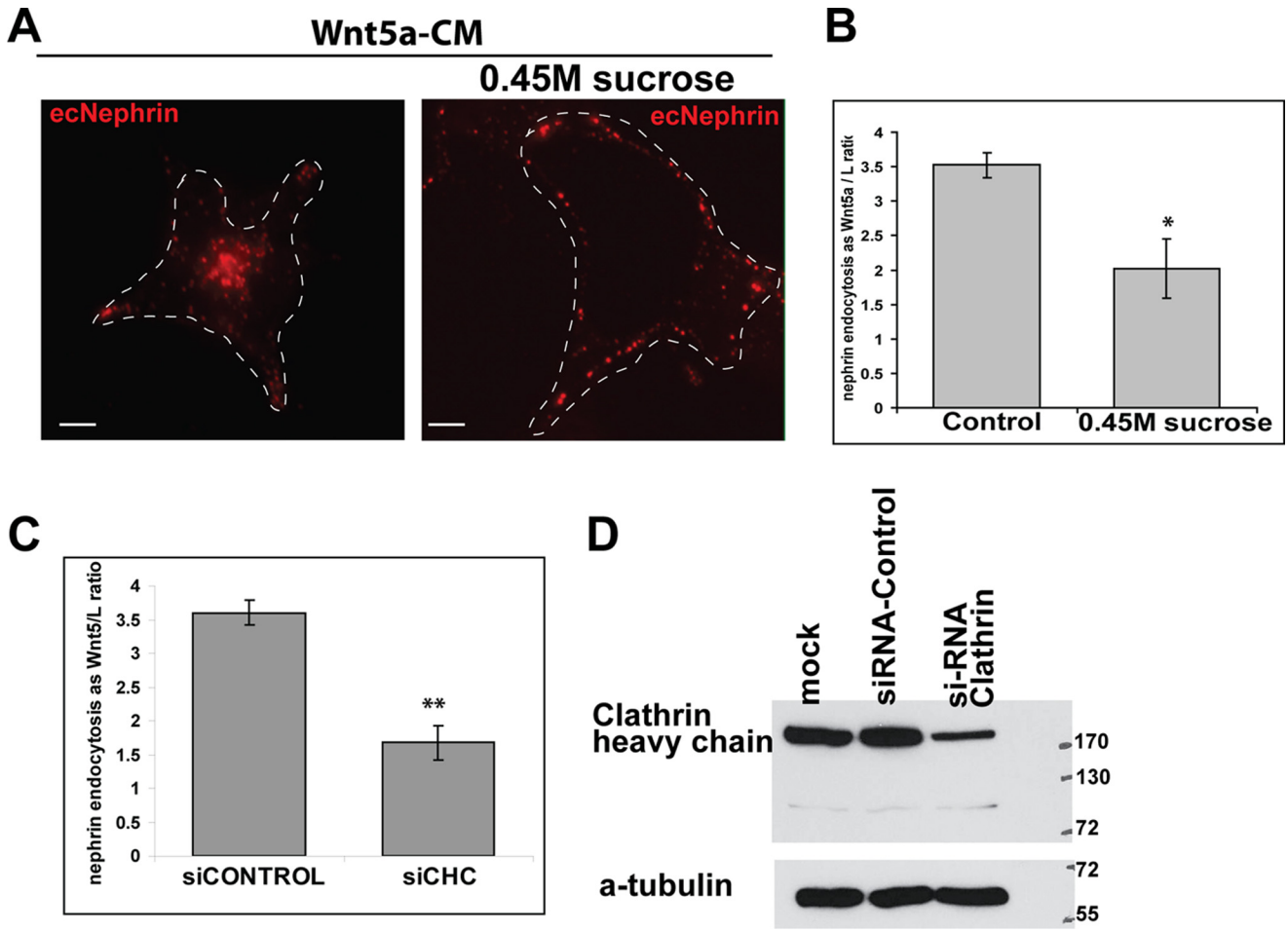

FIGURE 5. **Wnt5a induces nephrin endocytosis via a clathrin-dependent pathway.** *A*, HEK293/N cells incubated with Wnt5a (*left*) or pretreated with 0.45 M sucrose and then exposed to Wnt5a (*right*). The ectodomain of nephrin (*ecNephrin*, *red*) is visualized by mAb 5-1-6 labeling of live cells. *Scale bar*, 5 μm. *B*, ELISA quantification of nephrin endocytosis in HEK293/N cells incubated with Wnt5a or Wnt5a + 0.45 M sucrose. *, $p < 0.01$, *error bars*, S.E. *C*, ELISA quantification of nephrin endocytosis in HEK293/N cells transfected with either control siRNA or siRNAs against CHC. **, $p < 0.001$, *error bars*, S.E. All ELISAs were repeated three times in quadruplicate for each condition. The data are presented as the mean ratio of nephrin endocytosis in cells treated with Wnt5a-CM to cells treated with L-CM. *D*, immunoblot analysis (anti-CHC antibody) of lysates from mock transfected HEK293/N cells or cells transfected with siControl or siCHC RNAs. Immunoblotting with anti-α-tubulin antibody is used to monitor for equal loading.

PKCα (46). Thus, we tested whether Wnt5a augments nephrin endocytosis via PKCα. We pretreated HEK293/N cells with the 0.4 nM PKCα inhibitor prior to incubation with Wnt5a- or L-CM and performed ELISA as above. The PKCα inhibitor did not significantly reduce nephrin endocytosis induced by Wnt5a (3.69 ± 0.8-fold Wnt5a/L stimulation without PKCα inhibitor *versus* 2.84 ± 0.75-fold endocytosis stimulation) (Fig. 6*F*). Tested in parallel, the same concentration of PKCα inhibitor significantly ($p < 0.001$) reduced nephrin internalization induced by PMA (from 4.26 ± 0.13 down to 1.11 ± 0.12), indicating that the inhibitor was effective (Fig. 6*F*). Our results suggest that Wnt5a-induces β-arrestin-dependent nephrin endocytosis independently of PKCα.

Vangl2 Depletion Inhibits Nephrin Endocytosis—To test whether Wnt5a-stimulated nephrin endocytosis depends on the core PCP protein Vangl2, we depleted Vangl2 in the HEK293/N cells by transfecting the cells with anti-Vangl2 siRNAs. In the cells incubated with control L-CM, nephrin could be easily detected at the cell surface in the cells transfected with both control and anti-Vangl2 siRNA and live-labeled with mAb 5-1-6 (Fig. 7*A*, *upper panels*, *arrows*). In contrast, upon Wnt5-CM stimulation, nephrin became internalized in the cells transfected with siControl (Fig. 7*A*, *lower left panel*, *arrowheads*) but not with the siVangl2, where we detected a strong mAb 5-1-6-positive signal mainly at the cell surface (Fig. 7, *lower right panel*, *arrows*). Quantified by ELISA, the cells transfected with control siRNA displayed a 4.68 ± 0.46-fold Wnt5a/L increase in nephrin endocytosis, whereas Vangl2 depletion substantially suppressed nephrin endocytosis (1.44 ± 0.22-fold increase, Fig. 7*B*). Reduction in the level of nephrin internalization in siVangl2-treated cells correlated with the level of Vangl2 depletion measured by quantitative RT-PCR (Fig. 7*C*).

Loss of Vangl2 Affects Glomerular Maturation in Vivo—The *Looptail* (*Lp*) mouse harbors a spontaneous semidominant mutation in the *Vangl2* gene; homozygous *Lp* mice exhibit defects in multiple organs and die *in utero* of a severe neural tube defect in late gestation (17). We first analyzed the gross morphology of E17.5 embryonic kidneys from four homozygous *Lp/Lp* (Lp^{464} allele) embryos and matching wild-type littermates (Fig. 8, *A* and *B*). Compared with controls, *Lp/Lp* kidneys showed variable dysplasia, ranging from nearly normal

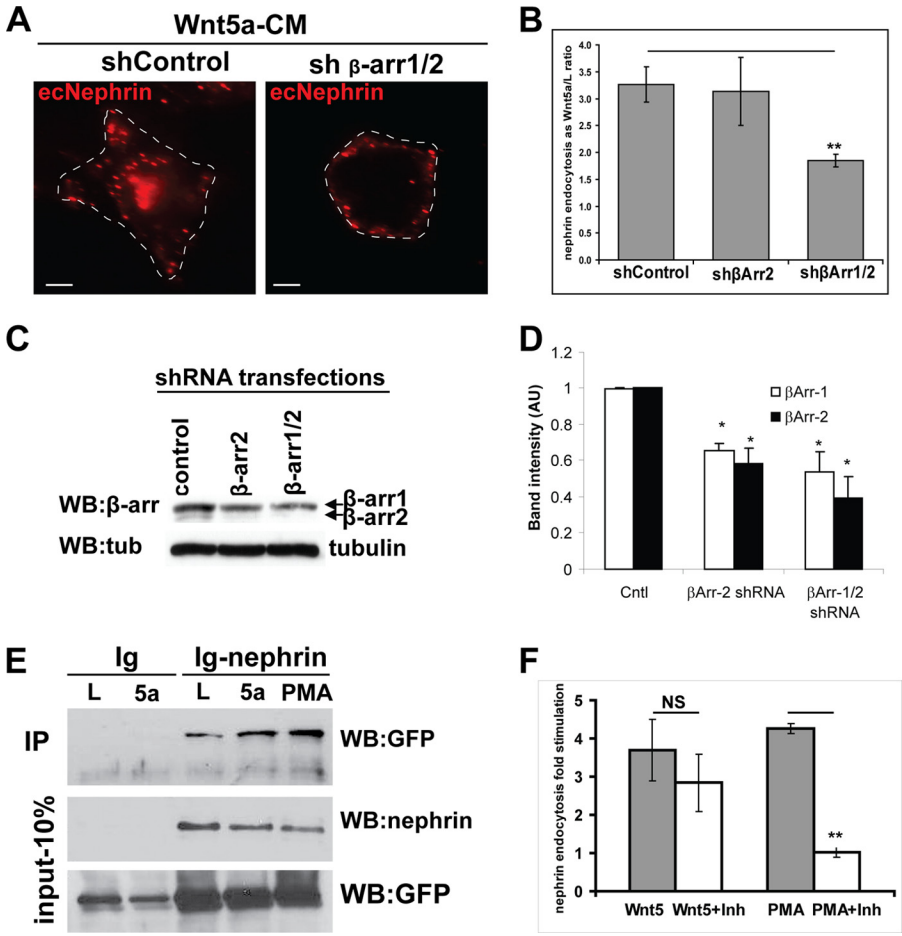

FIGURE 6. **Wnt5a stimulation of nephrin endocytosis depends on β-arrestins.** *A*, nephrin endocytosis inhibited in HEK293/N cells following knockdown of β-arrestin-1 and -2. *Left*, nephrin (mAb 5-1-6, *red*) detected in the cytoplasm of HEK293/N cells transfected with shControl and incubated with Wnt5a-CM. *Right*, nephrin (*red*) detected at the plasma membrane in cells transfected with shRNAs against β-arrestin-1/2 and incubated with Wnt5a. *Scale bar*, 5 μm. *B*, ELISAs in HEK293/N cells transfected with shRNAs against either control or β-arrestin-2 or a combination of β-arrestin-1 and -2. The ELISAs were repeated three times in quadruplicate for each condition. The data are presented as the ratio of nephrin endocytosis in cells treated with Wnt5a to L-CM. **, $p < 0.001$. *Error bars*, S.E. *C*, immunoblot (*WB*) analysis with pan-anti-β-arrestin antibodies in cells transfected with either control shRNA, or shRNA against β-arrestin-2 or shRNAs against both β-arrestin-1/2. Immunoblotting with anti-α-tubulin antibody is used to monitor for equal protein loading. Immunoblot analysis was repeated three times. *D*, densitometry quantification of immunoblotting analysis of β-arrestin expression from three different experiments. *, $p < 0.01$. *E*, pulldown assays between Ig-nephrin and Ig-control proteins and YFP-β-arrestin-2. All proteins were expressed in HEK293T cells that were treated for 3 h with either L- or Wnt5a or PMA (positive control). YFP-β-arrestin-2 was detected with anti-GFP antibody, Ig-nephrin was detected with polyclonal anti-nephrin antibody; pulldown experiments were repeated four times. *F*, densitometry quantification of pulldown experiments. **, $p < 0.001$.

shape to smaller flattened appearance (Fig. 8*A*, *right panel*). All *Lp/Lp* kidneys lacked clear demarcation between cortical and medullary zones and showed some degree of medullary hypoplasia with decreased evidence of tubular bundles and marked tubular dilation. Occasional glomerular cysts were seen (Fig. 8*B*).

Confocal microscopy of wild-type E17.5 kidneys showed that >60% of glomeruli were at the more mature 4–5 capillary loop-stage (Fig. 8, *C* and *D*). At this stage, podocytes (detected with antibody against Wilms tumor protein, WT1) express nephrin predominantly at the basal surface, corresponding to the position of slit diaphragm complexes (Fig. 8*C*, *right panels*). In contrast, we detected a significantly higher percentage of immature glomeruli (1–2 capillary loop-stage) in *Lp/Lp* kidneys (Fig. 8*D*). In immature glomeruli, nephrin expression is detected both at the basal and the lateral plasma membrane surfaces and occasionally in the apical membrane domains (Fig. 8*C*, *left panels*, *arrows*). The distribution of nephrin in mature glomeruli was similar in wild-type and *Lp/Lp* kidneys (Fig. 8*E*). The mean number of WT1-positive podocytes was similar in wild-type and *Lp/Lp* glomeruli at the 1–2 capillary loop-stage (21 *versus* 22 podocytes/glomerulus) and the 3–5 capillary loop-stage (19 *versus* 19 podocytes/glomerulus).

DISCUSSION

The noncanonical Wnt/PCP pathway is indispensible for mammalian organogenesis; defects in PCP genes cause abnormalities in multiple organs. In the kidney, our observations suggest that the PCP signaling is important for nephrin endocytosis and for glomerular maturation.

We identified a significant decrease in nephrin endocytosis in cultured podocytes with depleted Vangl2 expression and a significant developmental delay in glomerular maturation in *Vangl2* mutant *Lp* mice. Can Vangl2-regulated nephrin endocytosis contribute to podocyte and glomerular development and if so, how? The answer may reside in the known functions of the PCP pathway in lower organisms. During *Drosophila* wing development, a core PCP protein Flamingo (Fmi, atypical

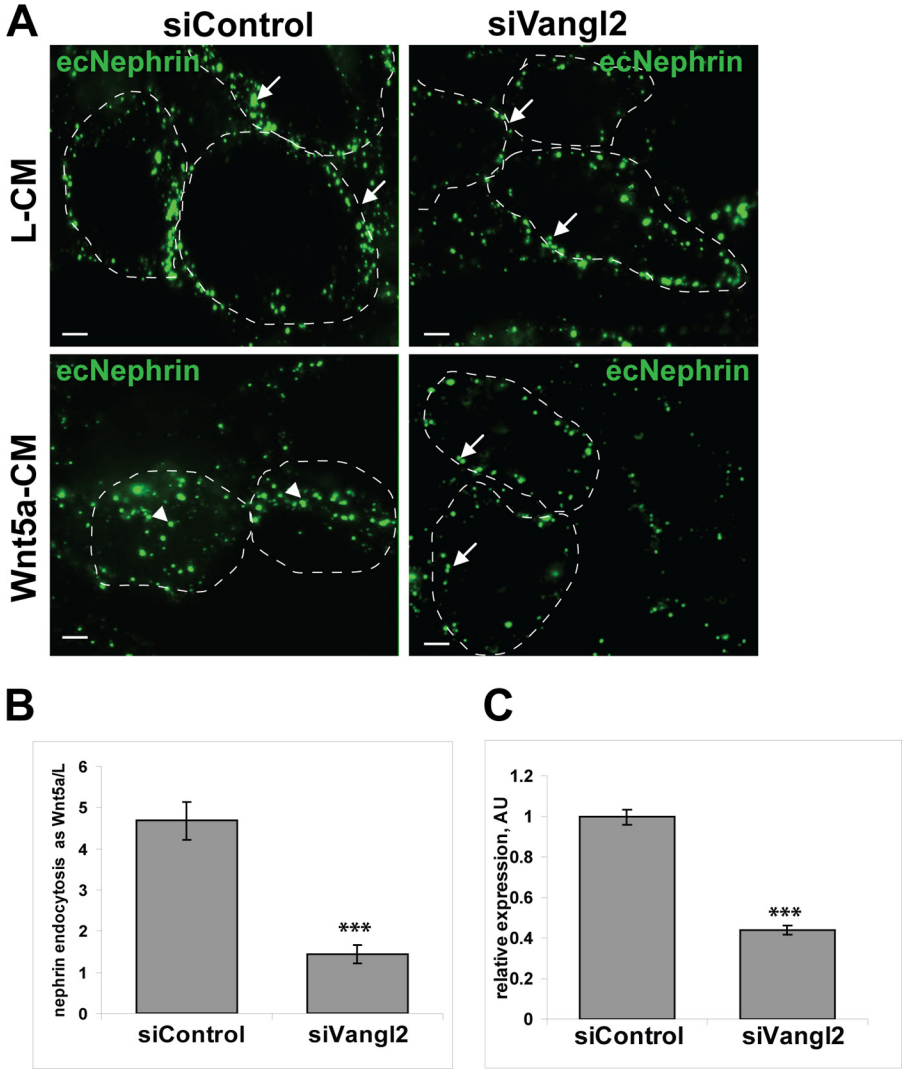

FIGURE 7. **Vangl2 mediates Wnt5a-stimulated nephrin endocytosis.** *A*, *upper panels*, HEK293/N cells transfected with either siControl or siVangl2 RNAs, live-labeled with mAb 5-1-6 and exposed to L-CM for 60 min. Nephrin (*green*) is mostly detected at the cell surface. *Lower panels*, HEK293/N cells transfected with either control or Vangl2 siRNAs, live-labeled with mAb 5-1-6, and incubated for 60 min with Wnt5a-CM. Note that nephrin (*green*) is mostly detected in the cytoplasm of the control siRNA-transfected cells but is localized primarily at the plasma membrane in the cells transfected with Vangl2 siRNA. *Scale bar*, 5 μm. *B*, ELISAs of Wnt5a-induced nephrin endocytosis in HEK293/N cells transfected with either siControl or siVangl2 RNAs. The ELISAs were repeated three times in quadruplicate for each condition. The data are presented as the ratio of nephrin endocytosis in cells treated with Wnt5a to cells treated with L-CM. ***, $p < 0.0001$. *Error bars*, S.E. *C*, quantitative RT-PCR of Vangl2 transcript in cells transfected with control or Vangl2 siRNAs. The experiment was repeated twice in triplicate. ***, $p < 0.0001$.

cadherin that possesses large extracellular domain) accumulates in discrete membrane domains that correspond to adherens junctions (47). Like nephrin, junction-associated Fmi interacts with Fmi from the adjacent cell to facilitate cell-cell adhesion. The PCP proteins Vang (a fly homologue of Vangl2) and Fz also concentrate in junctions and stabilize Fmi there; the unbound Fmi is actively endocytosed in a PCP-dependent manner via Rab5- and dynamin-dependent processes (48). In the absence of Vang and Fz, Fmi does not localize stably to the junctions and accumulates at the apical membrane at increased rate. This ultimately leads to the loss of asymmetric PCP protein complex assembly and loss of planar polarization (47). By analogy, Vangl2 may be critical for the proper localization of nephrin at the developing slit diaphragm via controlling its endocytosis.

There are several examples in which the PCP pathway regulates endocytosis of the "non-PCP" cell surface proteins. The PCP pathway was shown to control polarized endocytosis and recycling of E-cadherin during remodeling of wing cells (49) and tracheal elongation (50) in the fly. The repacking of wing epithelia involves growth and shrinkage of the plasma membrane plus assembly and disassembly of junctional complexes that allow cells to assume a hexagonal shape. This requires a dynamic PCP-dependent polarized turnover of E-cadherin at adherens junctions. In PCP mutants, level of E-cadherin at the junctions increases (49, 50). Similarly, tracheal elongation involves polarized cell intercalation that is accompanied by junctional remodeling and a decrease in E-cadherin at the junctions. Loss of PCP activity in PCP mutants (including *Vang*) leads to an increase in the stability and amount of E-cadherin in cell-cell junctions and a delay in tracheal branch intercalation (50). Another example can be drawn from the process of gastrulation during early vertebrate development. Gastrulation relies on the directional rearrangement of cellular cytoskeleton

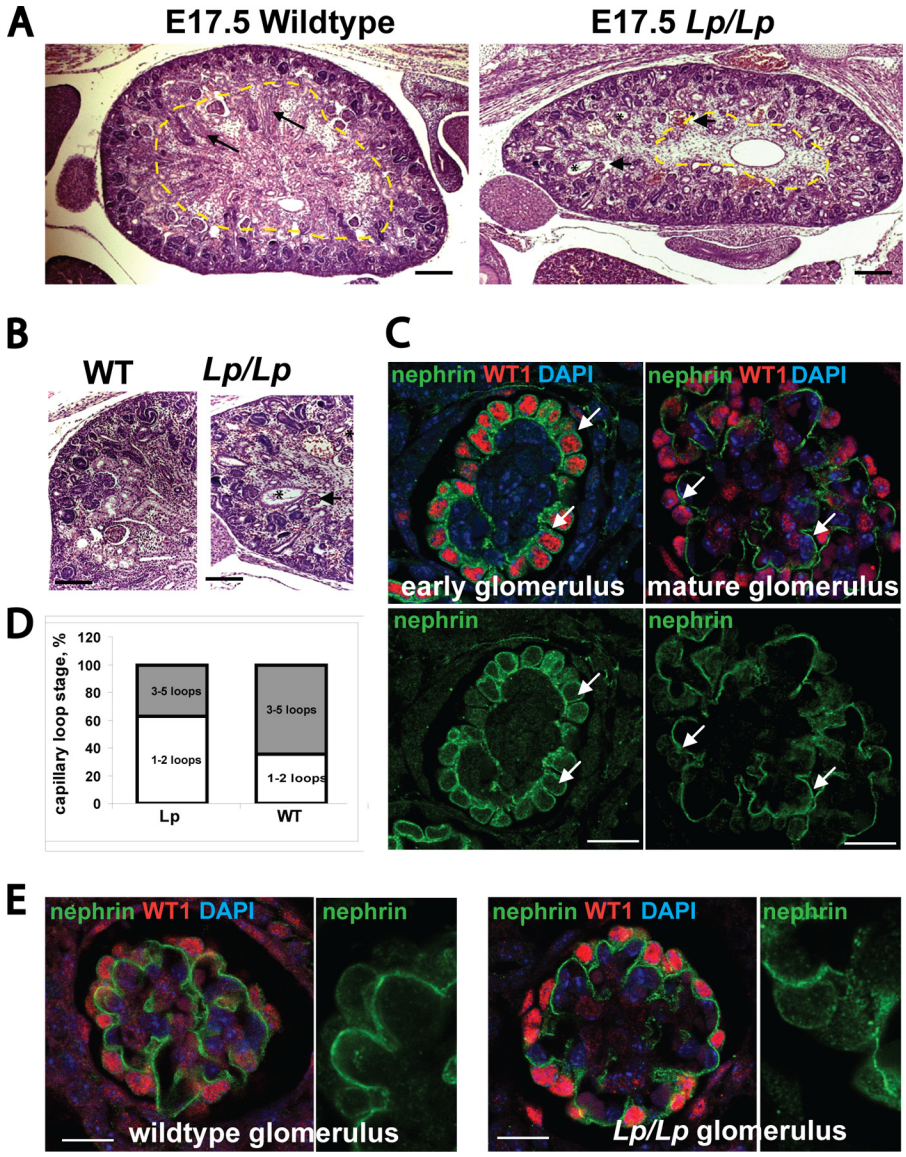

FIGURE 8. **Vangl2 *Looptail* (Vangl2) embryos exhibit defective glomerular maturation.** *A* and *B*, H&E staining of E17.5 wild-type (*left*) and *Lp/Lp* (*right*) kidneys. Cortical areas are designated by the *broken yellow line*, tubular bundles by *long arrows*, dilated tubules by (an *asterisk*), cystic glomeruli by *short arrows*. Note that images in *B* are from the same kidneys but not the same sections as shown in *A*. *Scale bars* are 50 and 20 μm. Four E17.5 *Lp/Lp* kidneys from different litters and four wild-type kidneys were analyzed. *C*, staging of glomerular maturation in E17.5 wild-type kidneys by confocal microscopy. *Upper panels*, merged images of double staining with guinea pig anti-nephrin antibody (*green*) and rabbit anti-WT1 antibody (*red*). In immature glomeruli at the one loop-stage (*left*), nephrin is detected along the entire lateral-basal and apical (*arrows*) surfaces. In mature glomeruli at the >5 loop-stage (*right*), nephrin is detected as a thin line exclusively at the basal podocyte surface. *Lower panels*, same images as above showing only the nephrin channel. *Scale bar*, 5 μm. *D*, quantification of glomerular developmental stage identified by nephrin/WT1 staining by confocal microscopy. More than 35 glomeruli were scored on sections prepared from two *Ll/Lp* and two wild-type (WT) E17.5 littermates from two different litters. *E*, nephrin (*green*), WT1 (*red*), and DAPI (*blue*) expression in maturing glomeruli of wild-type (*left*) and *Lp/Lp* (*right*) E17.5 embryonic kidneys. *Scale bar*, 5 μm. *Insets* show magnified images of nephrin (*green*) channel.

and convergent extension movements, processes controlled by the PCP pathway (1). During convergent extension in zebrafish, the PCP pathway regulates endocytosis of the metalloproteinase, MMP14, that is important for remodeling of extracellular matrix. Loss of *Vangl2* in *trilobite* mutants leads to a greater availability of MMP14 at the cell surface, disturbing normal extracellular matrix remodeling, miscoordination of polarized cell movements, and convergent extension defects (51). Vangl2 protein was shown to localize to the tips of filopodia in the commissural neuron axon growth cones (52) where it antagonized Wnt5-induced Fz3 phosphorylation and promoted Fz3 internalization. This allows "sharpening of PCP signaling locally on the tips of the filopodia to sense directional Wnt cues" (52). Thus, it is conceivable that Vangl2-mediated nephrin endocytosis has a critical role in the development of the highly specialized structure of podocytes.

To achieve their unique mature architecture, developing podocytes must remodel their membranes and junctional complexes extensively. We reported previously that Vangl2 interacts with nephrin via the SD scaffold protein MAGI2 and may be a part of the SD complex (20). Based on our observations, we propose that Vangl2 participates in the control of podocyte shape by internalizing nephrin prior to foot process formation and slit diaphragm junction assembly needed for terminal dif-

ferentiation. Conversely, loss of *Vangl2* may contribute to abnormal glomerular maturation in *Lp* mice by permitting premature nephrin externalization, disturbing podocyte alignment. The importance of endocytosis in glomerular development was recently demonstrated in transgenic mice lacking genes required for clathrin-dependent endocytic machinery (53): mutant mice with knockout of three *endophilin* genes or the *synaptojanin* failed to form normal foot processes and exhibited severe proteinuria and nephrotic syndrome at birth (53). These observations are in line with our results which show that loss of *Vangl2* function impairs glomerular maturation.

The robust Wnt5a-induced nephrin endocytosis we observed in the current study has several similarity to other systems; Wnt5a was previously reported to induce clathrin-mediated endocytosis of its receptors Fz4 (40), Fz2, and Ror2 (noncanonical Wnt/PCP co-receptor), where Fz internalization may be required for regulation of its receptor activity (8). Similarly, we established that depletion of clathrin heavy chain by siRNA interference or clathrin inhibition by sucrose substantially decreased Wnt5a-induced nephrin internalization. Wnt5a-induced endocytosis of Fz4 was reportedly modulated by β-arrestin-2 (40). Indeed, we also identified involvement of β-arrestins in the Wnt5a-induced nephrin endocytosis by demonstrating that siRNA knockdown of β-arrestin-1/2 led to a significance decrease in nephrin internalization. We also found that Wnt5a strengthened interactions between the nephrin cytoplasmic domain and β-arrestin-2. Thus, Wnt5a-induced endocytosis of nephrin appears to utilize a clathrin/β-arrestin-mediated endocytic pathway similar to Fz endocytosis. Quack *et al.* have also shown previously that nephrin is internalized via the clathrin/β-arrestin-2-dependent pathway in the high glucose milieu (27, 44).

Wnt5a-induced endocytosis of nephrin, however, displays some unique features. Chen *et al.* reported that, by itself, Wnt5a-CM was unable to trigger Fz4 endocytosis but that the combination of Wnt5a and the PKCα activator PMA led to Fz4 internalization (40). Quack also reported a requirement for PKCα activity to stimulate nephrin internalization in the presence of pathologic hyperglycemia (27). Our data do not support involvement of PKC for the following reasons: (i) Addition of a PKC inhibitor did not significantly decrease Wnt5a-stimulated nephrin endocytosis, whereas it efficiently inhibited PMA-stimulated nephrin internalization in the same experiment. (ii) Cell incubation with only Wnt5a was sufficient to increase nephrin internalization 3–5-fold without a requirement for PMA. (iii) Chen *et al.* did not see Wnt5a stimulation of complex formation between Fz4 and β-arrestin-2 (40). However, we detected an increase in nephrin/β-arrestin-2 interactions in the presence of Wnt5a. Taken together, our results demonstrate that Wnt5a stimulates PKC-independent nephrin internalization.

In HEK293/N cells stimulated with Wnt5a, we detected nephrin predominantly in Rab5 (early endosomes) and occasionally in Rab7 (late endosomes/early lysosomes)-positive vesicles but not in the Rab11 (recycling endosomal marker) vesicles. Rab5-mediated PCP-dependent endocytosis of Fmi and E-cadherin was also demonstrated in the fly wing cells (47) and zebrafish (54). The Rab7 endosomal compartment is usually associated with degradation of proteins such as EGF receptor (55). However, we did not detect any loss of nephrin in the Wnt5a-treated cells after 6 h. Although low undetectable amounts of nephrin may have escaped detection, our results are in line with previous studies of human podocytes in which we saw no loss of nephrin after 24 h of Wnt5a exposure (20). We, therefore, propose that Wnt5a causes a robust prolonged internalization of nephrin into endocytic vesicles, depleting the cell surface nephrin pool without marked nephrin degradation.

In adult kidneys, activation of the canonical Wnt pathway with subsequent β-catenin accumulation contributes to the podocyte dysfunction leading to proteinuria (56, 57). Although it was not the main focus of the study, Kato *et al.* also reported significant up-regulation of the noncanonical Wnts in the glomerulus affected by diabetic nephropathy in humans (Wnt4) and in rats (Wnt4 and Wnt5a) (57). Similarly, Wnt4 was up-regulated in the mouse model of adriamycin nephropathy, although the study was semiquantitative (56). Wnt5a does not stimulate β-catenin accumulation (supplemental Fig. 2); however, the above-mentioned reports, combined with our current results, suggest a possibility that inappropriate stimulation of Wnt5a in the adult kidney may lead to increased nephrin internalization, which would lead to SD destabilization and proteinuria. Whether the Wnt/PCP pathway is reactivated during podocyte injury is an important question that warrants further investigation.

In summary, we show that the noncanonical/PCP pathway stimulates PKC-independent, clathrin- and Rab5-mediated internalization of podocyte-specific adhesion protein nephrin. We propose that during glomerular development, PCP pathway signaling suppresses nephrin externalization prior to terminal podocyte differentiation. Conversely, a dysfunctional PCP pathway might affect glomerular maturation by permitting premature nephrin accumulation at adherens junctions to form slit diaphragms. In adult tissues, inappropriate Wnt5a expression may cause increased nephrin internalization leading to proteinuria.

Acknowledgments—We thank Dr. Philippe Gros (McGill) for providing Looptail mice, Dr. Samantha Gruenheid (McGill) for providing Rab5-GFP and Rab7-GFP plasmids, Dr. Moin Saleem (Bristol Children's Hospital) for a gift of human podocyte line A8/13, Dr. Stephane Laporte (McGill) for anti-β-arrestin-1/2 shRNAs and antibody, Dr. Peter McPherson for siRNA and antibody against CHC, and Dr. Ivo Quack for the Ig-nephrin and Ig-control expression constructs.

REFERENCES

1. Goodrich, L. V., and Strutt, D. (2011) Principles of planar polarity in animal development. *Development* **138,** 1877–1892
2. Heinonen, K. M., Vanegas, J. R., Lew, D., Krosl, J., and Perreault, C. (2011) Wnt4 enhances murine hematopoietic progenitor cell expansion through a planar cell polarity-like pathway. *PLoS One* **6,** e19279
3. Gao, B., Song, H., Bishop, K., Elliot, G., Garrett, L., English, M. A., Andre, P., Robinson, J., Sood, R., Minami, Y., Economides, A. N., and Yang, Y. (2011) Wnt signaling gradients establish planar cell polarity by inducing Vangl2 phosphorylation through Ror2. *Dev. Cell* **20,** 163–176
4. Karner, C. M., Chirumamilla, R., Aoki, S., Igarashi, P., Wallingford, J. B., and Carroll, T. J. (2009) Wnt9b signaling regulates planar cell polarity and kidney tubule morphogenesis. *Nat. Genet.* **41,** 793–799

5. Ye, X., Wang, Y., Rattner, A., and Nathans, J. (2011) Genetic mosaic analysis reveals a major role for Frizzled4 and Frizzled8 in controlling ureteric growth in the developing kidney. *Development* **138,** 1161–1172
6. Komiya, Y., and Habas, R. (2008) Wnt signal transduction pathways. *Organogenesis* **4,** 68–75
7. Carroll, T. J., and Yu, J. (2012) The kidney and planar cell polarity. *Curr. Top. Dev. Biol.* **101,** 185–212
8. Sato, A., Yamamoto, H., Sakane, H., Koyama, H., and Kikuchi, A. (2010) Wnt5a regulates distinct signalling pathways by binding to Frizzled2. *EMBO J.* **29,** 41–54
9. Wang, B., Sinha, T., Jiao, K., Serra, R., and Wang, J. (2011) Disruption of PCP signaling causes limb morphogenesis and skeletal defects and may underlie Robinow syndrome and brachydactyly type B. *Hum. Mol. Genet.* **20,** 271–285
10. Torban, E., Iliescu, A., and Gros, P. (2012) An expanding role of Vangl proteins in embryonic development. *Curr. Top. Dev. Biol.* **101,** 237–261
11. Fischer, E., Legue, E., Doyen, A., Nato, F., Nicolas, J. F., Torres, V., Yaniv, M., and Pontoglio, M. (2006) Defective planar cell polarity in polycystic kidney disease. *Nat. Genet.* **38,** 21–23
12. Luyten, A., Su, X., Gondela, S., Chen, Y., Rompani, S., Takakura, A., and Zhou, J. (2010) Aberrant regulation of planar cell polarity in polycystic kidney disease. *J. Am. Soc. Nephrol.* **21,** 1521–1532
13. Saburi, S., Hester, I., Fischer, E., Pontoglio, M., Eremina, V., Gessler, M., Quaggin, S. E., Harrison, R., Mount, R., and McNeill, H. (2008) Loss of Fat4 disrupts PCP signaling and oriented cell division and leads to cystic kidney disease. *Nat. Genet.* **40,** 1010–1015
14. Mao, Y., Mulvaney, J., Zakaria, S., Yu, T., Morgan, K. M., Allen, S., Basson, M. A., Francis-West, P., and Irvine, K. D. (2011) Characterization of a Dchs1 mutant mouse reveals requirements for Dchs1-Fat4 signaling during mammalian development. *Development* **138,** 947–957
15. Saburi, S., Hester, I., Goodrich, L., and McNeill, H. (2012) Functional interactions between Fat family cadherins in tissue morphogenesis and planar polarity. *Development* **139,** 1806–1820
16. Ciani, L., Patel, A., Allen, N. D., and French-Constant, C. (2003) Mice lacking the giant protocadherin mFAT1 exhibit renal slit junction abnormalities and a partially penetrant cyclopia and anophthalmia phenotype. *Mol. Cell. Biol.* **23,** 3575–3582
17. Kibar, Z., Vogan, K. J., Groulx, N., Justice, M. J., Underhill, D. A., and Gros, P. (2001) Ltap, a mammalian homolog of *Drosophila* Strabismus/Van Gogh, is altered in the mouse neural tube mutant *loop-tail*. *Nat. Genet.* **28,** 251–255
18. Strong, L. C., and Hollander, W. F. (1949) Hereditary *loop-tail* in the house mouse: accompanied by imperforate vagina and with lethal craniorachischisis when homozygous. *J. Hered.* **40,** 329–334
19. Yates, L. L., Papakrivopoulou, J., Long, D. A., Goggolidou, P., Connolly, J. O., Woolf, A. S., and Dean, C. H. (2010) The planar cell polarity gene *Vangl2* is required for mammalian kidney-branching morphogenesis and glomerular maturation. *Hum. Mol. Genet.* **19,** 4663–4676
20. Babayeva, S., Zilber, Y., and Torban, E. (2011) Planar cell polarity pathway regulates actin rearrangement, cell shape, motility, and nephrin distribution in podocytes. *Am. J. Physiol. Renal Physiol.* **300,** F549–560
21. Tryggvason, K. (1999) Unraveling the mechanisms of glomerular ultrafiltration: nephrin, a key component of the slit diaphragm. *J. Am. Soc. Nephrol.* **10,** 2440–2445
22. Khoshnoodi, J., Sigmundsson, K., Ofverstedt, L. G., Skoglund, U., Obrink, B., Wartiovaara, J., and Tryggvason, K. (2003) Nephrin promotes cell-cell adhesion through homophilic interactions. *Am. J. Pathol.* **163,** 2337–2346
23. Huber, T. B., and Benzing, T. (2005) The slit diaphragm: a signaling platform to regulate podocyte function. *Curr. Opin. Nephrol. Hypertens.* **14,** 211–216
24. Kestilä, M., Lenkkeri, U., Männikkö, M., Lamerdin, J., McCready, P., Putaala, H., Ruotsalainen, V., Morita, T., Nissinen, M., Herva, R., Kashtan, C. E., Peltonen, L., Holmberg, C., Olsen, A., and Tryggvason, K. (1998) Positionally cloned gene for a novel glomerular protein, nephrin, is mutated in congenital nephrotic syndrome. *Mol. Cell* **1,** 575–582
25. Greka, A., and Mundel, P. (2012) Cell biology and pathology of podocytes. *Annu. Rev. Physiol.* **74,** 299–323
26. Pierce, K. L., and Lefkowitz, R. J. (2001) Classical and new roles of β-arrestins in the regulation of G protein-coupled receptors. *Nat. Rev. Neurosci.* **2,** 727–733
27. Quack, I., Woznowski, M., Potthoff, S. A., Palmer, R., Königshausen, E., Sivritas, S., Schiffer, M., Stegbauer, J., Vonend, O., Rump, L. C., and Sellin, L. (2011) PKCα mediates β-arrestin-2-dependent nephrin endocytosis in hyperglycemia. *J. Biol. Chem.* **286,** 12959–12970
28. Tossidou, I., Teng, B., Drobot, L., Meyer-Schwesinger, C., Worthmann, K., Haller, H., and Schiffer, M. (2010) CIN85/RukL is a novel binding partner of nephrin and podocin and mediates slit diaphragm turnover in podocytes. *J. Biol. Chem.* **285,** 25285–25295
29. Qin, X. S., Tsukaguchi, H., Shono, A., Yamamoto, A., Kurihara, H., and Doi, T. (2009) Phosphorylation of nephrin triggers its internalization by raft-mediated endocytosis. *J. Am. Soc. Nephrol.* **20,** 2534–2545
30. Saleem, M. A., O'Hare, M. J., Reiser, J., Coward, R. J., Inward, C. D., Farren, T., Xing, C. Y., Ni, L., Mathieson, P. W., and Mundel, P. (2002) A conditionally immortalized human podocyte cell line demonstrating nephrin and podocin expression. *J. Am. Soc. Nephrol.* **13,** 630–638
31. Li, H., Lemay, S., Aoudjit, L., Kawachi, H., and Takano, T. (2004) SRC-family kinase Fyn phosphorylates the cytoplasmic domain of nephrin and modulates its interaction with podocin. *J. Am. Soc. Nephrol.* **15,** 3006–3015
32. Zimmerman, B., Simaan, M., Lee, M. H., Luttrell, L. M., and Laporte, S. A. (2009) c-Src-mediated phosphorylation of AP-2 reveals a general mechanism for receptors internalizing through the clathrin pathway. *Cell. Signal.* **21,** 103–110
33. Nassoury, N., Blasiole, D. A., Tebon Oler, A., Benjannet, S., Hamelin, J., Poupon, V., McPherson, P. S., Attie, A. D., Prat, A., and Seidah, N. G. (2007) The cellular trafficking of the secretory proprotein convertase PCSK9 and its dependence on the LDLR. *Traffic* **8,** 718–732
34. Torban, E., Wang, H. J., Patenaude, A. M., Riccomagno, M., Daniels, E., Epstein, D., and Gros, P. (2007) Tissue, cellular and sub-cellular localization of the Vangl2 protein during embryonic development: effect of the *Lp* mutation. *Gene Expr. Patterns* **7,** 346–354
35. Czachorowski, M., Lam-Yuk-Tseung, S., Cellier, M., and Gros, P. (2009) Transmembrane topology of the mammalian Slc11a2 iron transporter. *Biochemistry* **48,** 8422–8434
36. Quaggin, S. E., and Kreidberg, J. A. (2008) Development of the renal glomerulus: good neighbors and good fences. *Development* **135,** 609–620
37. Huber, T. B., Hartleben, B., Winkelmann, K., Schneider, L., Becker, J. U., Leitges, M., Walz, G., Haller, H., and Schiffer, M. (2009) Loss of podocyte aPKCλ/ι causes polarity defects and nephrotic syndrome. *J. Am. Soc. Nephrol.* **20,** 798–806
38. Belotti, E., Puvirajesinghe, T. M., Audebert, S., Baudelet, E., Camoin, L., Pierres, M., Lasvaux, L., Ferracci, G., Montcouquiol, M., and Borg, J. P. (2012) Molecular characterisation of endogenous Vangl2/Vangl1 heteromeric protein complexes. *PLoS One* **7,** e46213
39. Qian, D., Jones, C., Rzadzinska, A., Mark, S., Zhang, X., Steel, K. P., Dai, X., and Chen, P. (2007) Wnt5a functions in planar cell polarity regulation in mice. *Dev. Biol.* **306,** 121–133
40. Chen, W., ten Berge, D., Brown, J., Ahn, S., Hu, L. A., Miller, W. E., Caron, M. G., Barak, L. S., Nusse, R., and Lefkowitz, R. J. (2003) Dishevelled 2 recruits β-arrestin-2 to mediate Wnt5A-stimulated endocytosis of Frizzled4. *Science* **301,** 1391–1394
41. Daukas, G., and Zigmond, S. H. (1985) Inhibition of receptor-mediated but not fluid-phase endocytosis in polymorphonuclear leukocytes. *J. Cell Biol.* **101,** 1673–1679
42. Oakley, R. H., Laporte, S. A., Holt, J. A., Barak, L. S., and Caron, M. G. (1999) Association of β-arrestin with G protein-coupled receptors during clathrin-mediated endocytosis dictates the profile of receptor resensitization. *J. Biol. Chem.* **274,** 32248–32257
43. Claing, A., Laporte, S. A., Caron, M. G., and Lefkowitz, R. J. (2002) Endocytosis of G protein-coupled receptors: roles of G protein-coupled receptor kinases and β-arrestin proteins. *Prog. Neurobiol.* **66,** 61–79
44. Quack, I., Rump, L. C., Gerke, P., Walther, I., Vinke, T., Vonend, O., Grunwald, T., and Sellin, L. (2006) β-Arrestin-2 mediates nephrin endocytosis and impairs slit diaphragm integrity. *Proc. Natl. Acad. Sci. U.S.A.* **103,** 14110–14115
45. Sellin, L., Huber, T. B., Gerke, P., Quack, I., Pavenstädt, H., and Walz, G.

(2003) NEPH1 defines a novel family of podocin interacting proteins. *FASEB J.* **17,** 115–117
46. Yang, D. H., Yoon, J. Y., Lee, S. H., Bryja, V., Andersson, E. R., Arenas, E., Kwon, Y. G., and Choi, K. Y. (2009) Wnt5a is required for endothelial differentiation of embryonic stem cells and vascularization via pathways involving both Wnt/β-catenin and protein kinase Cα. *Circ. Res.* **104,** 372–379
47. Strutt, H., and Strutt, D. (2008) Differential stability of Flamingo protein complexes underlies the establishment of planar polarity. *Curr. Biol.* **18,** 1555–1564
48. Strutt, H., Warrington, S. J., and Strutt, D. (2011) Dynamics of core planar polarity protein turnover and stable assembly into discrete membrane subdomains. *Dev. Cell* **20,** 511–525
49. Classen, A. K., Anderson, K. I., Marois, E., and Eaton, S. (2005) Hexagonal packing of *Drosophila* wing epithelial cells by the planar cell polarity pathway. *Dev. Cell* **9,** 805–817
50. Warrington, S. J., Strutt, H., and Strutt, D. (2013) The Frizzled-dependent planar polarity pathway locally promotes E-cadherin turnover via recruitment of RhoGEF2. *Development* **140,** 1045–1054
51. Williams, B. B., Cantrell, V. A., Mundell, N. A., Bennett, A. C., Quick, R. E., and Jessen, J. R. (2012) VANGL2 regulates membrane trafficking of MMP14 to control cell polarity and migration. *J. Cell Sci.* **125,** 2141–2147
52. Shafer, B., Onishi, K., Lo, C., Colakoglu, G., and Zou, Y. (2011) Vangl2 promotes Wnt/planar cell polarity-like signaling by antagonizing Dvl1-mediated feedback inhibition in growth cone guidance. *Dev. Cell* **20,** 177–191
53. Soda, K., Balkin, D. M., Ferguson, S. M., Paradise, S., Milosevic, I., Giovedi, S., Volpicelli-Daley, L., Tian, X., Wu, Y., Ma, H., Son, S. H., Zheng, R., Moeckel, G., Cremona, O., Holzman, L. B., De Camilli, P., and Ishibe, S. (2012) Role of dynamin, synaptojanin, and endophilin in podocyte foot processes. *J. Clin. Invest.* **122,** 4401–4411
54. Ulrich, F., Krieg, M., Schötz, E. M., Link, V., Castanon, I., Schnabel, V., Taubenberger, A., Mueller, D., Puech, P. H., and Heisenberg, C. P. (2005) Wnt11 functions in gastrulation by controlling cell cohesion through Rab5c and E-cadherin. *Dev. Cell* **9,** 555–564
55. Vanlandingham, P. A., and Ceresa, B. P. (2009) Rab7 regulates late endocytic trafficking downstream of multivesicular body biogenesis and cargo sequestration. *J. Biol. Chem.* **284,** 12110–12124
56. Dai, C., Stolz, D. B., Kiss, L. P., Monga, S. P., Holzman, L. B., and Liu, Y. (2009) Wnt/β-catenin signaling promotes podocyte dysfunction and albuminuria. *J. Am. Soc. Nephrol.* **20,** 1997–2008
57. Kato, H., Gruenwald, A., Suh, J. H., Miner, J. H., Barisoni-Thomas, L., Taketo, M. M., Faul, C., Millar, S. E., Holzman, L. B., and Susztak, K. (2011) Wnt/β-catenin pathway in podocytes integrates cell adhesion, differentiation, and survival. *J. Biol. Chem.* **286,** 26003–26015